

## Identification of an immunogenic neo-epitope encoded by mouse sarcoma using CXCR3 ligand mRNAs as sensors

Keisuke Fujii, Yoshihiro Miyahara, Naozumi Harada, Daisuke Muraoka, Mitsuhiro Komura, Rui Yamaguchi, Hideo Yagita, Junko Nakamura, Sahoko Sugino, Satoshi Okumura, Seiya Imoto, Satoru Miyano & Hiroshi Shiku

To cite this article: Keisuke Fujii, Yoshihiro Miyahara, Naozumi Harada, Daisuke Muraoka, Mitsuhiro Komura, Rui Yamaguchi, Hideo Yagita, Junko Nakamura, Sahoko Sugino, Satoshi Okumura, Seiya Imoto, Satoru Miyano & Hiroshi Shiku (2017) Identification of an immunogenic neo-epitope encoded by mouse sarcoma using CXCR3 ligand mRNAs as sensors, *OncoImmunology*, 6:5, e1306617, DOI: [10.1080/2162402X.2017.1306617](https://doi.org/10.1080/2162402X.2017.1306617)

To link to this article: <https://doi.org/10.1080/2162402X.2017.1306617>



© 2017 The Author(s). Published with license by Taylor & Francis Group, LLC© Keisuke Fujii, Yoshihiro Miyahara, Naozumi Harada, Daisuke Muraoka, Mitsuhiro Komura, Rui Yamaguchi, Hideo Yagita, Junko Nakamura, Sahoko Sugino, Satoshi Okumura, Seiya Imoto, Satoru Miyano, and Hiroshi Shiku



[View supplementary material](#)



Accepted author version posted online: 20 Mar 2017.  
Published online: 20 Mar 2017.



[Submit your article to this journal](#)



Article views: 495



[View related articles](#)



[View Crossmark data](#)

ORIGINAL RESEARCH

 OPEN ACCESS



## Identification of an immunogenic neo-epitope encoded by mouse sarcoma using CXCR3 ligand mRNAs as sensors

Keisuke Fujii<sup>a</sup>, Yoshihiro Miyahara<sup>a</sup>, Naozumi Harada<sup>a</sup>, Daisuke Muraoka<sup>a,b</sup>, Mitsuhiro Komura<sup>c</sup>, Rui Yamaguchi<sup>c</sup>, Hideo Yagita<sup>d</sup>, Junko Nakamura<sup>a</sup>, Sahoko Sugino<sup>a</sup>, Satoshi Okumura<sup>a</sup>, Seiya Imoto<sup>e</sup>, Satoru Miyano<sup>c</sup>, and Hiroshi Shiku<sup>a</sup>

<sup>a</sup>Department of Immuno-Gene Therapy, Graduate School of Medicine, Mie University, Mie, Japan; <sup>b</sup>Center for Drug Discovery, Graduate School of Pharmaceutical Sciences, University of Shizuoka, Shizuoka, Japan; <sup>c</sup>Laboratory of DNA Information Analysis, Human Genome Center, Institute of Medical Science, University of Tokyo, Tokyo, Japan; <sup>d</sup>Department of Immunology, Juntendo University School of Medicine, Tokyo, Japan; <sup>e</sup>Division of Health Medical Data Science, Health Intelligence Center, Institute of Medical Science, University of Tokyo, Tokyo, Japan

### ABSTRACT

The CXCR3 ligands CXCL9, 10, and 11 play critical roles in the amplification of immune responses by recruiting CXCR3<sup>+</sup> immune effector cells to the tumor site. Taking advantage of this property of CXCR3 ligands, we aimed to establish a novel approach to identify immunogenic mutated-antigens. We examined the feasibility of using CXCR3 ligand mRNAs as sensors for detection of specific immune responses in human and murine systems. We further investigated whether this approach is applicable for the identification of immunogenic mutated-antigens by using murine sarcoma lines. Rapid synthesis of CXCR3 ligand mRNAs occurred shortly after specific immune responses in both human and murine immune systems. Particularly, in CMS5 tumor-bearing mice, we detected specific immune responses to mutated mitogen-activated protein kinase 2 (ERK2), which has previously been identified as an immunogenic mutated-antigen. Furthermore, by combining this approach with whole-exome and transcriptome sequencing analyses, we identified an immunogenic neo-epitope derived from mutated staphylococcal nuclease domain-containing protein 1 (Snd1) in CMS7 tumor-bearing mice. Most importantly, we successfully detected the specific immune response to this neo-epitope even without co-administration of anti-cytotoxic T-lymphocyte protein-4 (CTLA-4), anti-programmed cell death-1 (PD-1) and anti-glucocorticoid-induced TNFR-related protein (GITR) antibodies, which vigorously augmented the immune response and consequently enabled us to detect the specific immune response to this neo-epitope by conventional IFN $\gamma$  intracellular staining method.

Our data indicate the potential usefulness of this strategy for the identification of immunogenic mutated-antigens. We propose that this approach would be of great help for the development of personalized cancer vaccine therapies in future.

### ARTICLE HISTORY

Received 23 December 2016  
Revised 26 February 2017  
Accepted 9 March 2017

### KEYWORDS

Checkpoint blockade; CXCR3 ligands; immune response; mutated antigen; neo-epitope


## Introduction

Cellular immune responses against mutated antigens originating from somatic genomic alterations occurring in an individual's tumor play critical roles in controlling and eradicating tumors.<sup>1-3</sup> One line of evidence supporting this notion comes from recent advances in immune checkpoint blockade therapies, which utilize monoclonal antibodies (mAbs) targeting CTLA-4 and PD-1.<sup>1,4-6</sup> Although the precise mechanism by which these antibodies exert their effect is still not fully understood, animal and human clinical studies indicate that neo-antigen specific autologous T cells, activated by these checkpoint inhibitors, play critical roles in killing tumor cells and impeding tumor growth. This concept is further supported by the fact that tumors with a high load of somatic mutations are more likely to respond to this therapy.<sup>5,7,8</sup>

A second line of evidence supporting the role of immune responses against mutated tumor antigens for cancer treatment comes from adoptive tumor-infiltrating lymphocyte (TIL) therapy that has been used for treating patients with melanoma and a patient with cholangiocarcinoma.<sup>9,10</sup> These serial studies have also emphasized the significance of mutated antigen-specific T cells by showing that the frequency and number of these T cells among the expanded TILs were closely correlated with the clinical efficacy of the treatment.

Collectively, these results indicate that mutated antigens are key target antigens recognized by autologous T cells, which can cause a substantial reduction in tumor burden. Given that immune responses against mutated antigens directly correlate with a positive clinical outcome, it is important to better understand the biologic interactions between the host immune system and the mutated antigens to develop more effective

**CONTACT** Yoshihiro Miyahara  [miyahy@clin.medic.mie-u.ac.jp](mailto:miyahy@clin.medic.mie-u.ac.jp); Hiroshi Shiku  [shiku@clin.medic.mie-u.ac.jp](mailto:shiku@clin.medic.mie-u.ac.jp) 

 Supplemental data for this article can be accessed on the [publisher's website](#).

Published with license by Taylor & Francis Group, LLC © Keisuke Fujii, Yoshihiro Miyahara, Naozumi Harada, Daisuke Muraoka, Mitsuhiro Komura, Rui Yamaguchi, Hideo Yagita, Junko Nakamura, Sahoko Sugino, Satoshi Okumura, Seiya Imoto, Satoru Miyano, and Hiroshi Shiku.

This is an Open Access article distributed under the terms of the Creative Commons Attribution-NonCommercial-NoDerivatives License (<http://creativecommons.org/licenses/by-nc-nd/4.0/>), which permits non-commercial re-use, distribution, and reproduction in any medium, provided the original work is properly cited, and is not altered, transformed, or built upon in any way.

immunotherapies; hence, it has become increasingly important to analyze cellular immune responses against the mutated antigens and identify the immunogenic neo-epitopes that could be potentially used as ideal targets for immunotherapies. Indeed, advanced techniques in next-generation sequencing have enabled us to rapidly identify genomic mutations. However, it has been laborious to identify populations of very rare mutated antigens, which are able to elicit immune responses *in vivo*, from among a numerous number of candidate antigens. Although several screening approaches, such as using synthetic mRNAs simultaneously expressing multiple antigens,<sup>11</sup> mass-spectrometry-based techniques<sup>12</sup> or tetramer-based conditional UV-mediated peptide exchange technology,<sup>13</sup> have been explored to overcome this obstacle, identifying immunogenic epitopes remains challenging.

In this study, we aimed at establishing an alternative strategy for the identification of immunogenic neo-epitopes by using CXCR3 ligand mRNAs as rapid indicators of specific immune responses. Although the methodology using CXCR3 ligand mRNA as an indicator of immune responses has been established by Chakera et al.,<sup>14</sup> we hypothesized that improvement of this method would enable us to simultaneously analyze immune responses against several synthetic neo-epitope peptides in a short time of period. We determined the feasibility of this approach in multiple models of human and murine immune response. By combining this approach with whole-exome and transcriptome sequencing analyses, we were able to identify immunogenic neo-epitopes encoded by the murine fibro-sarcoma cell line CMS7.

## Results

### *CXCR3 ligand mRNAs are sensitive indicators of specific immune responses*

The first aim of our study was to determine whether CXCR3 ligands are appropriate molecular indicators of specific immune response. For this purpose, we first used a model of the human cellular immune response against the immunogenic cancer/testis antigen NY-ESO-1.<sup>15</sup> After retroviral transduction with an  $\alpha/\beta$  TCR (T cell receptor) that can recognize the NY-ESO-1<sub>p157-165</sub> epitope (SLLMWITQC) in an HLA-A0201 restricted manner (Fig. 1A),<sup>16</sup> human CD8<sup>+</sup> T cells were incubated overnight with the NY-ESO-1 expressing melanoma cell line 397mel or with 397melA0201, a cell line derived from 397mel that stably expresses HLA-A0201. Subsequently, the levels of cytokines and chemokines in the culture media were evaluated using the BioPlex system, which enables simultaneous determination of the levels of 48 different cytokines and chemokines, excluding CXCL11. We found that the protein levels of nine molecules, including CXCL9, CXCL10, and IFN $\gamma$  substantially increased in an HLA-A0201 dependent manner (Fig. 1B).

We verified that the same phenomenon also occurred in a human immune response model against Epstein-Barr (EB) virus, which elicits CD8<sup>+</sup> T-cell immune responses in infected individuals. As previously reported, CD8<sup>+</sup> T cells recognizing the immunogenic EB nuclear antigen 3A (EBNA3A)-derived 9-mer peptide (RYSIFFDYM) in an HLA-A24-restricted fashion are found in the peripheral blood of latently infected with EB virus HLA-A24<sup>+</sup> donors.<sup>17</sup> Following an overnight incubation

of peripheral blood mononuclear cells (PBMC) of latently infected with EB virus HLA-A24<sup>+</sup> donors in the presence of either this peptide or the control, DMSO, the levels of the same 9 proteins in the culture media increased in an antigen-dependent manner (Fig. S1).

We next tested whether synthesis of mRNA encoding these proteins was rapidly triggered by antigenic stimulation, which could be used for the sensitive detection of a specific immune response. Following the addition of the antigenic peptide, we periodically extracted whole cell RNA and quantified the fold increase in the RNA levels of the nine selected cytokines/chemokines, in addition to CXCL11, compared with the DMSO control. As expected, a rapid increase in the mRNA expression of CXCR3 ligands was detected as early as 3 h following the peptide addition, whereas only a minor increase of IFN $\gamma$  mRNA expression was detected during the time periods examined (Fig. 1C). This marked increase in mRNA expression was dependent not only on the peptide epitope, but also on HLA-A24 expression, as indicated by the lack of such an increase in PBMC from a HLA-A24<sup>-</sup> donor latently infected with EB virus (Fig. S2).

### *The kinetics of mRNA synthesis of the CXCR3 ligands differs with the long peptide*

We hypothesized that the kinetics of mRNA synthesis might be different for the long (> 20-mer) peptide that is often used in immunogenic neo-epitope searching. To test this possibility using the same experimental setting as described above, we incubated PBMC derived from HLA-A24<sup>+</sup> donors latently infected with EB virus with the long peptide (20-mer), which included the EBNA3A 9-mer short peptide in its center. As expected, it took as long as 8 h following the peptide addition for CXCL9 mRNA expression to reach maximum levels. Again, we observed a minor increase in IFN $\gamma$  mRNA expression during the time periods examined (Fig. 2A).

To determine whether this phenomenon is similarly observed in a different model of human immune response, we used PBMC from one patient, from which we had previously established an HLA-B35-restricted NY-ESO-1<sub>p94-104</sub> specific CTL clone. After the addition of the NY-ESO-1<sub>p91-110</sub> 20-mer peptide containing the NY-ESO-1<sub>p94-104</sub> epitope to the cells, we periodically quantified the fold increase in mRNA levels of the CXCR3 ligands compared with the DMSO control. As expected, it also took as long as 8 h for mRNA expression of these chemokines to reach maximum levels (Fig. 2B), while we observed no increase in the synthesis of CXCR3 ligand mRNAs when using HLA-35<sup>+</sup> PBMC from a healthy donor (data not shown). These observations might be explained by the possibility that it takes more time for the long peptide to be processed and presented on the cell surface of antigen presenting cells.

### *This method is applicable to murine immune systems as well*

We tested the applicability of our method to the murine immune system as well, by using DUC18 TCR transgenic mice, expressing an  $\alpha/\beta$  TCR gene derived from a CD8<sup>+</sup> T-cell clone, which recognizes a mutated mitogen-activated protein kinase 2 (ERK2)-derived neo-epitope (mERK2-9m) presented by H-2K<sup>d</sup>

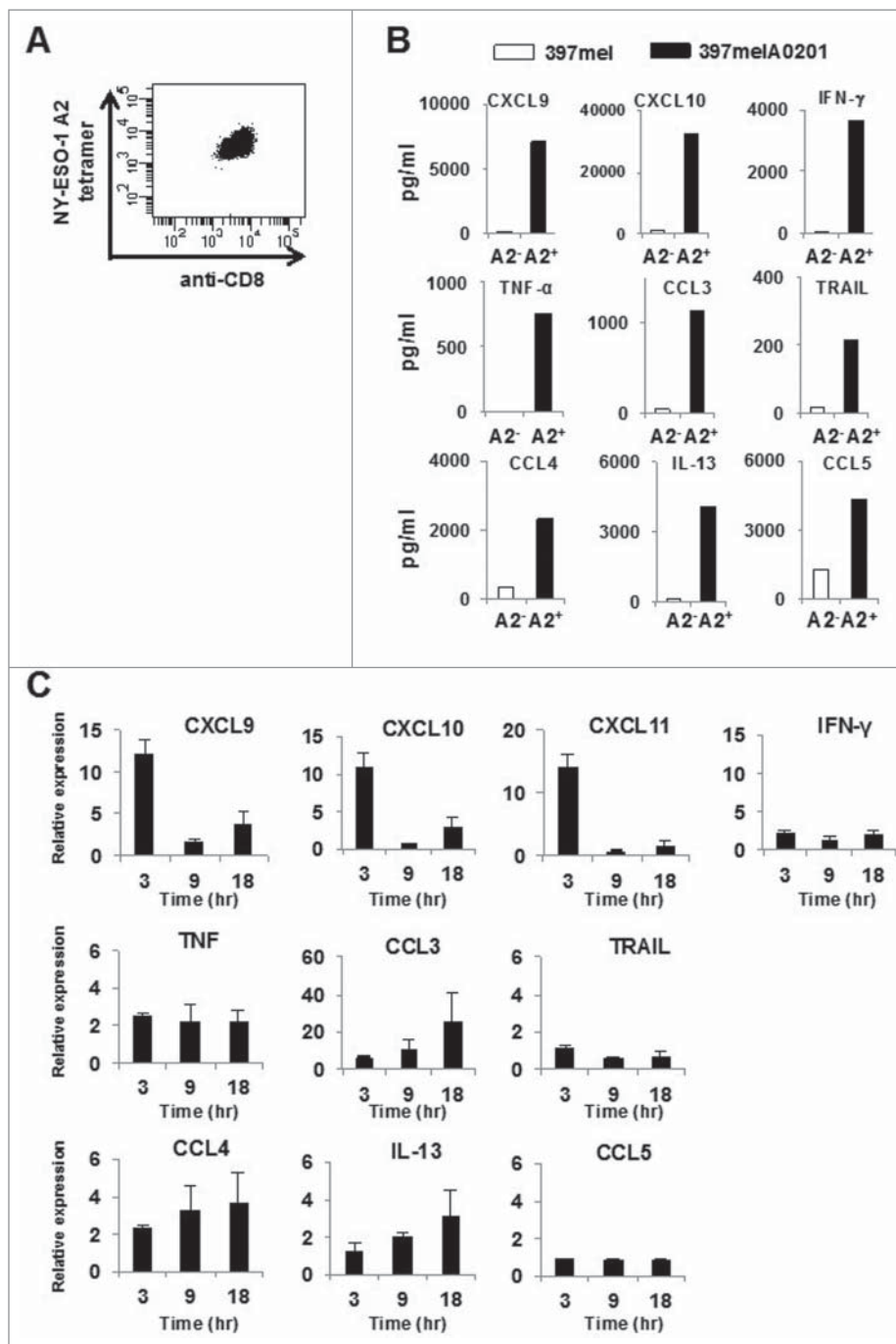


**Figure 1.** CXCR3 ligand mRNAs are sensitive indicators of specific immune responses. (A) Peripheral blood T cells from a healthy donor were expanded *in vitro* and retrovirally transduced with the NY-ESO-1<sub>p157-165</sub>/HLA-A0201-specific TCR. The CD8<sup>+</sup> T cells positively stained by the NY-ESO-1<sub>p157-165</sub>/A0201 tetramer were isolated by sorting. (B) Following overnight incubation of NY-ESO-1<sub>p157-165</sub> specific CD8<sup>+</sup> T cells with 397mel or 397melA0201, the levels of 48 cytokines/chemokines in the culture supernatants were evaluated using the Bio-Plex system. Data for nine selected cytokines/chemokines that increased in an HLA-A2 dependent manner are shown. (C) PBMC from A24<sup>+</sup> donors latently infected with EB virus were stimulated with EBNA3A<sub>246-254</sub> (RYSIFFDYM) peptide or DMSO as a control, and total RNA was extracted at the indicated time points. The fold increase of mRNA levels of the nine selected cytokines/chemokines and of CXCL11 compared with the DMSO control was evaluated by RT-qPCR. Expression of each gene was normalized to that of GAPDH. One representative data set out of three independent experiments is shown. Data represent relative quantity means  $\pm$  SD.

on the cell surface of murine fibro-sarcoma cell line CMS5.<sup>18,19</sup> We mixed  $1 \times 10^6$  splenic cells from wild-type BALB/c mice with  $2 \times 10^2$  splenic cells from DUC18 mice, and following the addition of the mERK2-9m peptide or the wERK2-9m peptide, we periodically quantified the fold increase in mRNA levels of the murine CXCR3 ligands compared with the DMSO control. As shown in Fig. 3A, we observed significant increases in the mRNA expression of murine CXCR3 ligands as early as 5 h

following the mERK2-9m peptide addition, similarly to human CXCR3 ligands (Fig. 3A).

We then tested whether the long (> 20-mer) peptide is also applicable to the murine immune system. We immunized BALB/c mice with the protein-based vaccine CHP-NY-ESO-1, twice at a 1-week interval,<sup>20</sup> and prepared splenic cell suspensions from pooled spleens one week following the last vaccination. Each peptide (20-25-mer) from 17 overlapping peptides



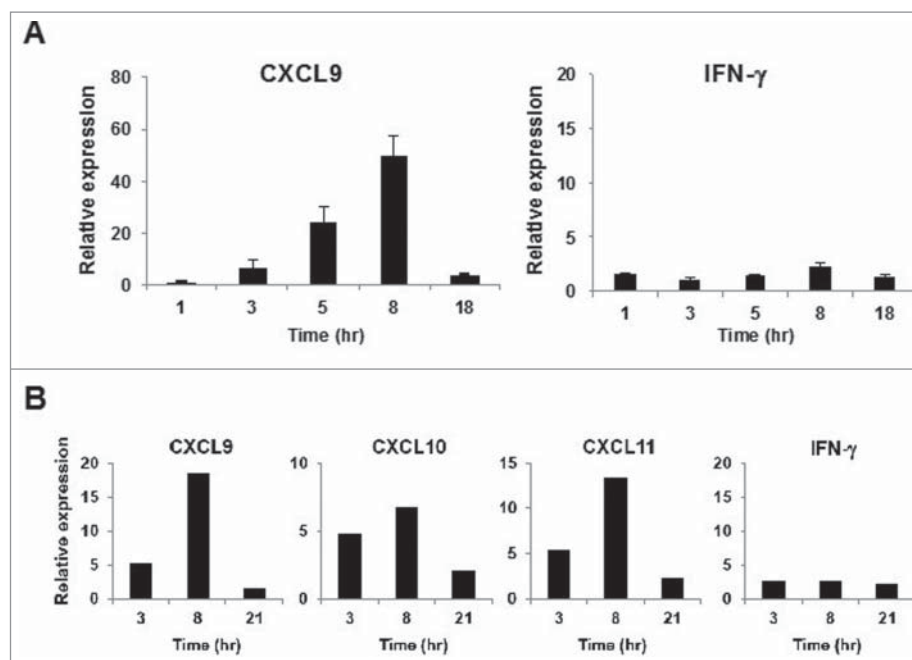


**Figure 2.** Kinetics of CXCR3 ligand mRNA synthesis following treatment with long peptides. (A) PBMC from A24<sup>+</sup> donors latently infected with EB virus were stimulated with EBNA3A<sub>240–259</sub> (20-mer; VQSCNPRYSIFFDYMAIHRHS) peptide or DMSO as a control. Relative fold increase of mRNA levels of CXCL9 and IFN $\gamma$  compared with the DMSO control was evaluated by RT-qPCR. One representative data out of three independent experiments is shown. Data represent relative quantity means  $\pm$  SD. (B) In this experiment, we used the same PBMC aliquot from which we had previously established an HLA-B35 restricted NY-ESO-1<sub>p94–104</sub> peptide specific CTL clone. After addition of NY-ESO-1<sub>p91–110</sub> (20-mer) peptide or DMSO as a control, total RNA was extracted from PBMC at the indicated time points. The relative fold increase of mRNA levels of CXCL9 and IFN $\gamma$  compared with DMSO control was quantified.

spanning the entire amino acid sequence of NY-ESO-1 (Table S1) or DMSO as a control were added to splenic cells from immunized mice, and the fold increase in murine CXCL9 mRNA levels was quantified following an 8-h incubation. We observed that murine CXCL9 mRNA expression significantly increased after the addition of 2 distinct peptides, NY-ESO-1<sub>p71–90</sub> and NY-ESO-1<sub>p81–100</sub> (Fig. 3B). Interestingly, the data show that both peptides contained the identical 9-mer epitope, NY-ESO-1<sub>p81–88</sub> (RGPE SRL L), which is the immunogenic and unique epitope recognized by murine CD8<sup>+</sup> T cells in an H-2D<sup>d</sup>-restricted manner, as our group has previously reported.<sup>21</sup>

Collectively, we concluded that our method is applicable for the detection of specific immune responses in the murine system as well.

#### Rapid synthesis of CXCR3 ligand mRNAs after low IFN $\gamma$ secretion by CD8<sup>+</sup> T cells

Although mRNA synthesis of the CXCR3 ligand appears to respond rapidly to specific immune responses than synthesis of IFN $\gamma$  mRNA, CXCR3 ligands are well-known IFN $\gamma$  inducible proteins. To determine the effect of IFN $\gamma$ , we periodically quantified the protein levels of CXCL9, CXCL10, and IFN $\gamma$  in the same culture medium after the addition of the EBNA3A 9-mer peptide to PBMC from HLA-A24<sup>+</sup> donors latently infected with EB virus. We observed that CXCL9 and CXCL10 in the culture medium became detectable shortly after the peptide addition, whereas IFN $\gamma$  was not detectable at the indicated time points (Fig. 4A). However, the robust increase in CXCL9 mRNA expression was completely diminished when we blocked IFN $\gamma$  signaling by the addition of anti-IFN $\gamma$  or anti-IFN $\gamma$  receptor neutralizing antibodies into the culture medium

(Fig. 4B). Moreover, IFN $\gamma$  secreted by CD8<sup>+</sup> T cells was essential for the robust synthesis of CXCL9 ligand mRNA, since we could not detect an increase in CXCL9 mRNA expression when CD8<sup>+</sup> T cells from IFN $\gamma$  knockout DUC18 mice were co-cultured with wild-type BALB/c splenic cells that were pulsed with the mERK2-9m peptide (data not shown). An increase in CXCL9 mRNA expression was detected when using the control IFN $\gamma$  competent DUC18 mice. Similar to the murine immune system, we found that CXCL9 mRNA synthesis was also diminished in the immune response model against EB virus when we used CD8<sup>+</sup>-depleted PBMC instead of whole PBMC (Fig. 4C and D). These data suggest that CD8<sup>+</sup> T cells capable of producing IFN $\gamma$  exist in peripheral blood, although we cannot detect such IFN $\gamma$  producing CD8<sup>+</sup> T cells in PBMCs by IFN $\gamma$  ICS assay before incubation with EBNA3A<sub>246–254</sub> peptide for a certain period of time (Fig. S3). Furthermore, we also observed the same phenomenon when we used CD14<sup>+</sup>-depleted PBMC (Fig. S4), as has been previously reported.<sup>14,22</sup> Taken together, these results clearly indicate that the minute amount of IFN $\gamma$  secreted by CD8<sup>+</sup> T cells is sufficient and essential for CD14<sup>+</sup> cells to rapidly and robustly produce CXCR3 ligands at both the protein and mRNA levels.

#### Detection of CD8<sup>+</sup> T-cell immune responses against tumors in tumor-bearing mice

To determine whether our method was sufficiently sensitive to detect CD8<sup>+</sup> T-cell immune responses against tumors in tumor-bearing mice, we used at first the murine colorectal tumor cell line CT26 which expresses the murine leukemia virus (MuLV) gp70-derived dominant CD8<sup>+</sup> T-cell epitope AH-1.<sup>23</sup> In pooled spleen cells, isolated 2 weeks after the

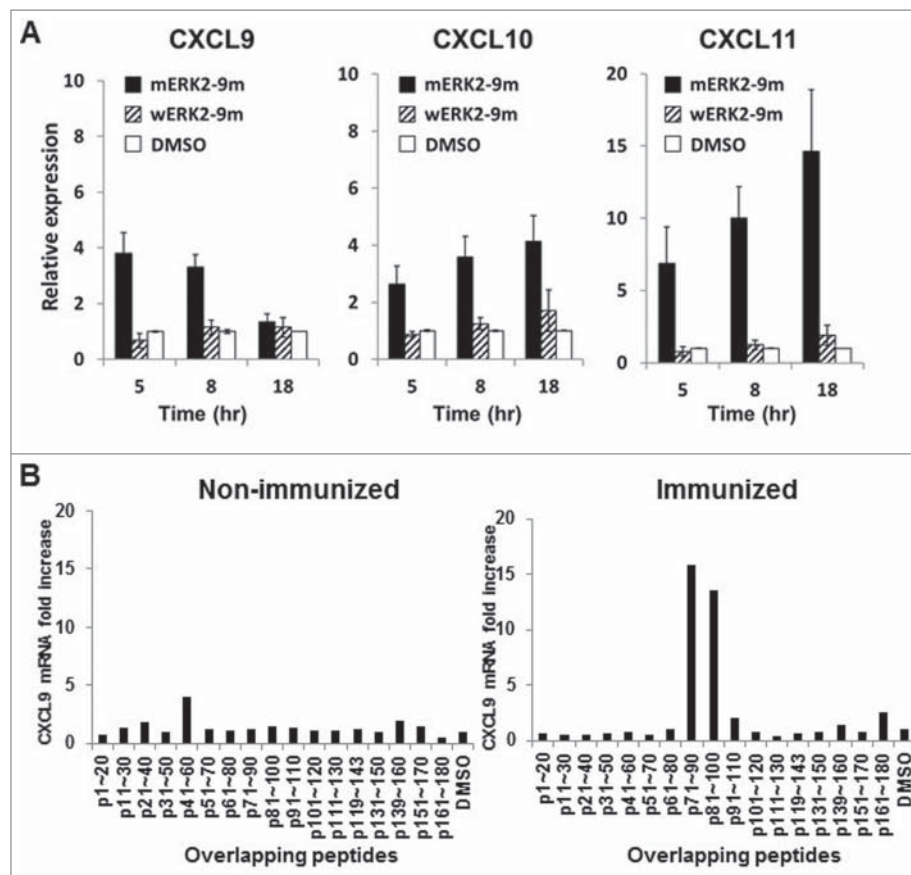


**Figure 3.** Kinetics of CXCR3 ligand mRNA synthesis are similar in murine and human immune system. (A) Splenocytes from naive BALB/c mice were mixed with splenocytes isolated from DUC18 mice. Mixed splenocytes were incubated with mERK2-9m peptide, wERK2-9m peptide or DMSO as a control. The relative fold increase of mRNA levels of murine CXCL9 compared with the DMSO control was quantified by RT-qPCR at the indicated time points. (B) CHP-NY-ESO-1 was subcutaneously injected into the back of BALB/c mice, twice at a 1-week interval. Splenic cells from pooled spleens ( $n = 3$  per experiment) were prepared for analysis 7 d after the second immunization. Pooled splenic cells from naive BALB/c (left) or immunized BALB/c (right) mice were incubated with one of 17 overlapping peptides spanning the whole amino acid sequence of NY-ESO-1 (Table S1) or DMSO as a control for 8 h. Total RNA was extracted, and the relative fold increase of mRNA levels of murine CXCL9 compared with DMSO was quantified.

subcutaneous administration of CT26 tumor cells into the flanks of BALB/c mice, we added the AH1 or mERK2-9m peptides, or DMSO as a control, and quantified the fold increase in CXCL9 mRNA levels following a 5-h incubation. As shown in Fig. 5A, we successfully detected a specific immune response to AH-1, as indicated by the significant increase in CXCL9 mRNA expression observed only following the addition of the AH-1 peptide.

Subsequently, we investigated whether we could detect neo-epitope-specific CD8<sup>+</sup> T-cell immune responses in tumor-bearing mice. To this end, we used the murine fibro-sarcoma cell line CMS5, which expresses the immunogenic neo-epitope, mERK2-9m, following the same procedure as described for the CT26 cell line. In pooled spleen cells isolated from CMS5 tumor-bearing mice, we added the mERK2-9m or AH-1 peptides, or DMSO as a control, and quantified the fold increase in CXCL9 mRNA levels. However, no significant increase in CXCL9 mRNA expression was observed in any of the conditions tested (data not shown). Recent advances in immunology indicate that the administration of immune-stimulating agonistic antibodies, such as anti-GITR antibody and anti-CD40 antibody, can also augment cellular immune responses against tumors, as well as checkpoint blockade antibodies. Based on this information, we tested whether immune responses to the

mERK2-9m peptide became detectable following intra-peritoneal administration of anti-CTLA-4, PD-1 and GITR antibodies. Indeed, under these conditions, we successfully detected a specific immune response to mERK2-9m, as indicated by the significant increase of CXCL9 mRNA synthesis observed only following mERK2-9m addition (Fig. 5B). However, a specific immune response to this neo-epitope was not detected by the IFN $\gamma$  intracellular staining (ICS) and IFN $\gamma$  ELISPOT assay regardless of the antibody treatment (Fig. 5C and D). These data suggest that our method can detect immune responses only of a certain magnitude, although it seems to be more sensitive than IFN $\gamma$  ICS or IFN $\gamma$  ELISPOT assay.

#### Successful identification of an immunogenic neo-epitope encoded by mouse sarcoma CMS7

By combining whole-exome and transcriptome sequencing analyses, we aimed at identifying tumor immunogenic neo-epitopes using the murine fibro-sarcoma cell line CMS7. To this end, we identified nonsynonymous somatic point mutations specifically expressed in the tumor by comparing exome sequencing data of CMS7 tumors with that of BALB/c mice tails. Then, transcriptome sequencing data were applied to deduce the expression potential of the mutated antigens at the

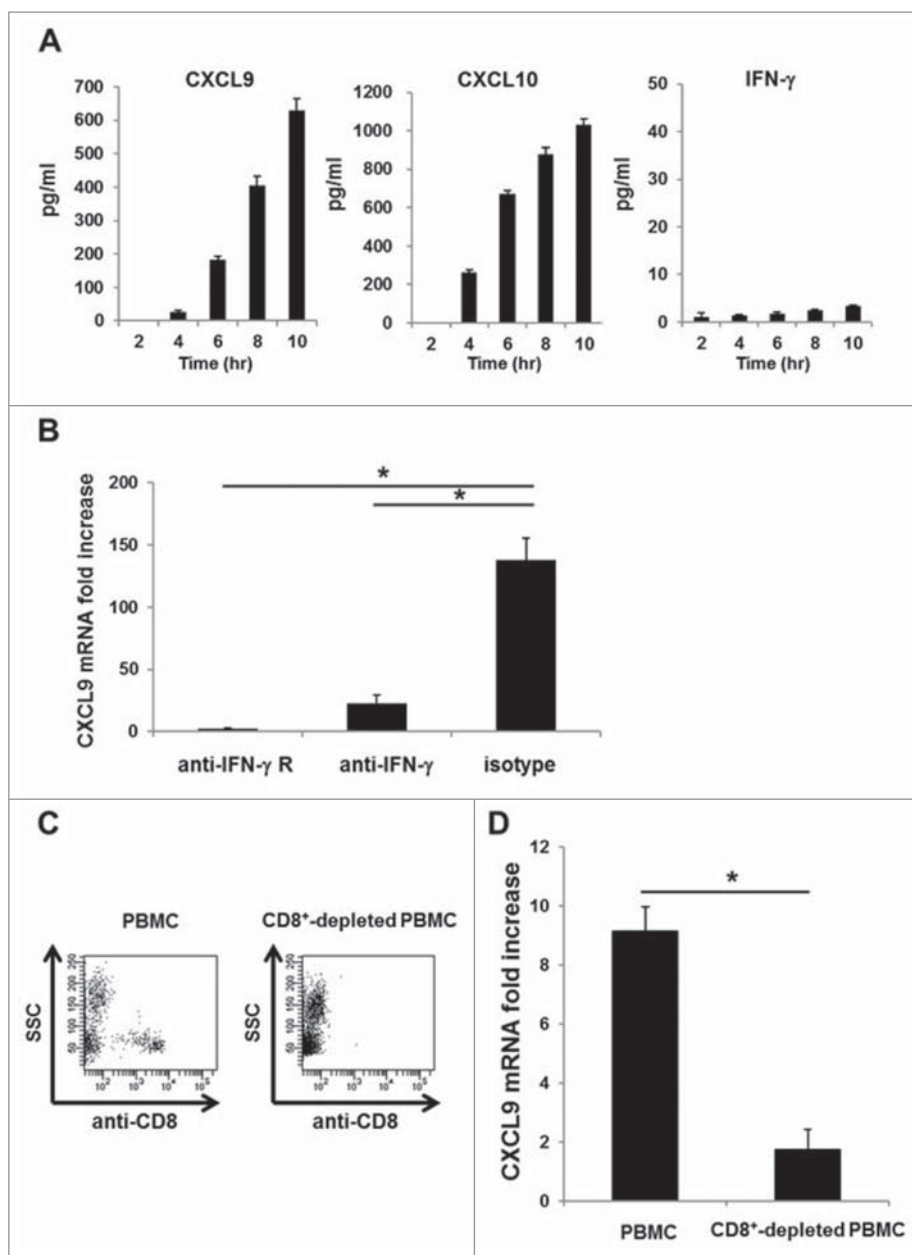


**Figure 4.** A minute amount of IFN $\gamma$  secreted by CD8<sup>+</sup> T cells is sufficient to induce rapid and robust CXCR3 ligand mRNA synthesis. (A) PBMC from A24<sup>+</sup> donors latently infected with EB virus were incubated with EBNA3A<sub>246–254</sub> peptide. At the indicated time points, the levels of CXCL9, CXCL10 and IFN $\gamma$  in the culture supernatant were evaluated by ELISA. One representative data out of three independent experiments using different PBMC donors is shown. Data represent means  $\pm$  SD. (B) Blocking assay, whereby PBMC from A24<sup>+</sup> donors latently infected with EB virus were cultured for 1 h in the presence of an anti-IFN $\gamma$  receptor mAb, an anti-IFN $\gamma$  mAb or an isotype control mAb before incubation with EBNA3A<sub>246–254</sub> peptide or DMSO as a control. After 5-h incubation with EBNA3A<sub>246–254</sub> peptide, the relative fold increase of mRNA levels of CXCL9 compared with DMSO was quantified. Data represent relative quantity means  $\pm$  SD. Asterisks indicate statistically significant differences ( $p < 0.01$ ). (C) Flow cytometry analysis before (left) and after (right) cell sorting. The CD8<sup>+</sup> population was depleted from PBMC by cell sorting. (D) Each population was incubated with EBNA3A<sub>246–254</sub> peptide. The relative fold increase in mRNA levels of CXCL9 over the DMSO control was quantified. Data represent relative quantity means  $\pm$  SD. Asterisks indicate statistically significant difference ( $p < 0.01$ ).

protein level. Complete lists of mutation-containing peptides, each ranging from 8 to 10 amino acids, were prepared and filtered based on their predicted binding affinities to each of the murine H-2K<sup>d</sup>, D<sup>d</sup>, or L<sup>d</sup> alleles using the IEDB analysis resource ([http://tools.immuneepitope.org/analyze/html/mhc\\_binding.html](http://tools.immuneepitope.org/analyze/html/mhc_binding.html)). Finally, we prepared a total of 57 candidate neo-epitope peptides encoded by CMS7 (Table 1), and evaluated their immunogenicity using splenic cells derived from CMS7 tumor-bearing mice as described below.

BALB/c mice were subcutaneously inoculated with CMS7 tumor cells in their flanks at day 0 and were divided into two

groups. One group was left untreated, while in the other anti-CTLA-4, anti-PD-1 and anti-GITR antibodies were intraperitoneally administered at days 7, 9, and 11. At day 21, the two groups of mice were sacrificed and splenic cell suspensions were prepared from pooled spleens. Following the addition of a panel of neo-epitope peptides or DMSO as a control to splenic cells, the specific immune response to each peptide was measured by our method. In both mouse groups, we observed a significant increase in CXCL9 mRNA levels following the addition of only a single neo-epitope derived from mutated Snd1 (staphylococcal nuclease domain-containing protein 1)

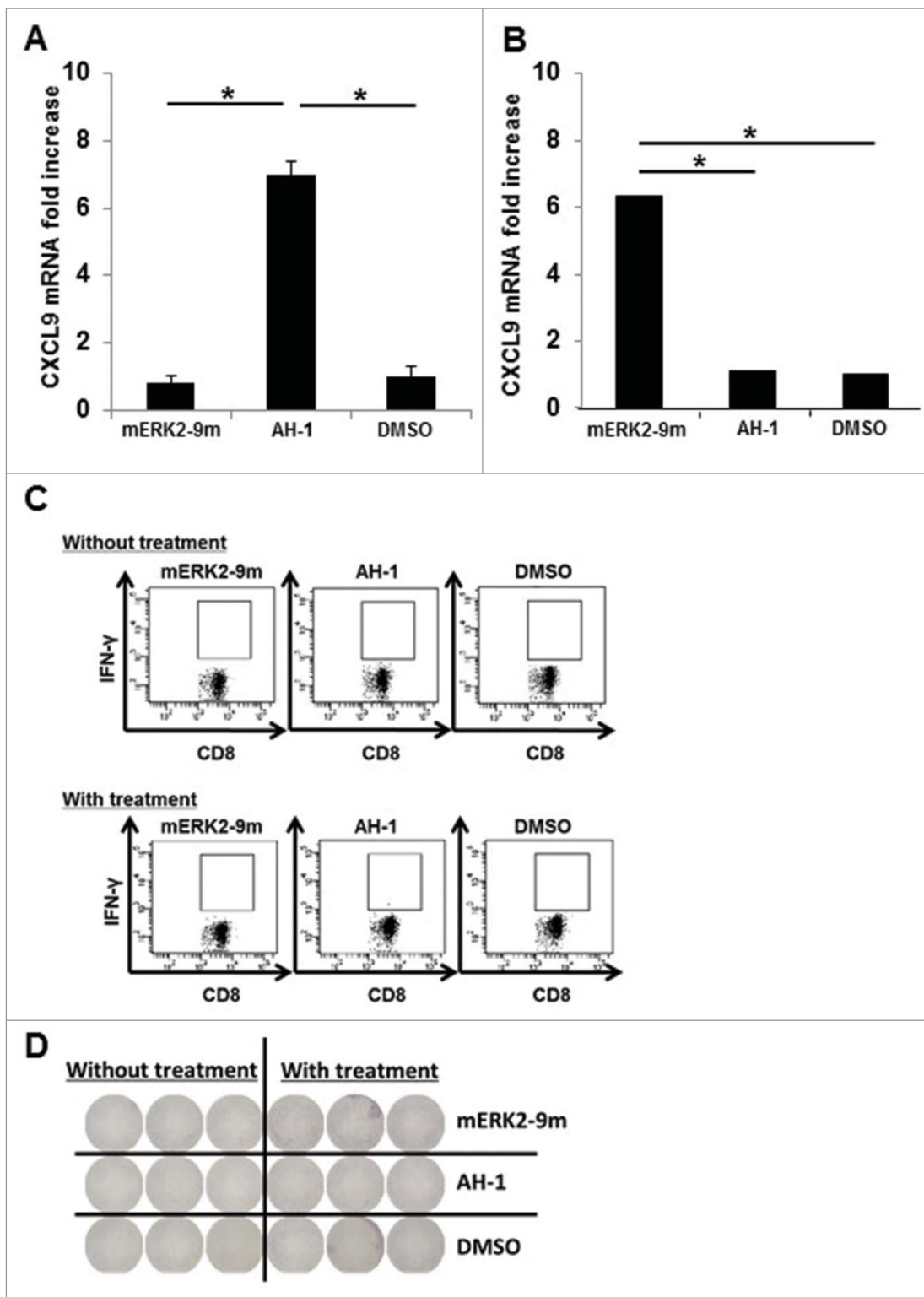


**Figure 5.** Detection of cellular immune responses against tumors in tumor-bearing mice. (A) Splenocytes from CT26 tumor-bearing BALB/c mice were incubated with mERK2-9m peptide, AH1 peptide, or DMSO as a control. The relative fold increase in mRNA levels of murine CXCL9 compared with DMSO was quantified 5 h later. One representative data out of three independent experiments is shown. Data represent relative quantity means  $\pm$  SD. Asterisks indicate statistically significant differences ( $p < 0.01$ ). (B) After subcutaneous inoculation with  $1 \times 10^6$  CMS5 cells, mice were randomly divided into 2 groups. One group was left untreated, and the other was intraperitoneally administered with 100  $\mu$ g of anti-CTLA-4, 200  $\mu$ g of anti-PD-1 and 150  $\mu$ g of anti-GITR mAbs at days 7, 9, and 11. Both mouse groups were sacrificed at day 21 and splenic cell suspensions were prepared from pooled spleens ( $n = 3$  per experiment). Splenic cells ( $1 \times 10^6$ ) from the antibody-treated group were incubated with mERK2-9m peptide, AH1 peptide, or DMSO as a control. The relative fold increase in mRNA levels of murine CXCL9 compared with DMSO was quantified 5 h later. One representative data set out of three independent experiments is shown. Data represent relative quantity means  $\pm$  SD. Asterisks indicate statistically significant differences ( $p < 0.01$ ). (C) For IFN $\gamma$  intracellular staining, splenic cells from both mouse groups were incubated with mERK2-9m peptide, AH1 peptide or DMSO as a control for 15 min at room temperature, and subsequently with GolgiPlug for 4 h. Following stimulation, cells were stained for cell surface CD8 $^+$  and intracellular IFN $\gamma$ . Representative dot plots gated on CD8 $^+$  splenocytes were shown. These experiments were repeated three times with similar results. (D) Pooled splenic cells from antibody treated or untreated CMS5 tumor-bearing mice were subjected to IFN $\gamma$  ELISPOT assays. Pooled splenic cells were incubated *in vitro* with mERK2-9m, AH-1 or DMSO for 18 h. One representative data out of three independent experiments is shown.



**Table 1.** The list of candidate neo-epitopes encoded by CMS7 tumor.

ID	length	peptide	Allele	IC50 (nM)	Symbol	n Change	a.a.Change	Entrez gene name
C7-1	10	RGPLNLFETC	H-2-Dd	2854	Plekhg5	c.G176T	p.C59F	pleckstrin homology domain containing, family G (with RhoGef domain) member 5
C7-2	8	VPPAALRL	H-2-Ld	101	Anapc2	c.G157C	p.G53R	anaphase promoting complex subunit 2
C7-3	8	TPLNIAL	H-2-Ld	64	Gba	c.G325C	p.A109P	glucosidase, beta, acid
C7-4	8	LPVATVTL	H-2-Ld	98	Il6ra	c.G119T	p.G40V	interleukin 6 receptor, alpha
C7-5	8	YAPCRGEF	H-2-Dd	1371	Snd1	c.C2191T	p.R731C	staphylococcal nuclease and tudor domain containing 1
C7-6	8	LPACKFQL	H-2-Ld	95	Trappc6a	c.G460T	p.V154L	trafficking protein particle complex 6A
C7-7	9	SPYQPKYGF	H-2-Ld	47	Trim12c	c.A1193C	p.H398P	tripartite motif-containing 12C
C7-8	8	VPAEALSF	H-2-Ld	98	Dnase2a	c.G65T	p.C22F	deoxyribonuclease II alpha
C7-9	10	QYAPAAPSEV	H-2-Kd	248	2810004N23Rik	c.C266A	p.S89Y	RIKEN cDNA 2810004N23 gene
C7-10	8	CGPLKLLV	H-2-Dd	1399	Supv311	c.C710T	p.A237V	suppressor of var1, 3-like 1 (S. cerevisiae)
C7-11	8	YPNRFLHM	H-2-Ld	42	Gnptab	c.G3503C	p.R1168P	N-acetylglucosamine-1-phosphate transferase, alpha and beta subunits
C7-12	8	IPFCLQSF	H-2-Ld	44	Gls2	c.G659T	p.C220F	glutaminase 2 (liver, mitochondrial)
C7-13	9	LYLPMVQSV	H-2-Kd	23	Dazap2	c.C224T	p.A75V	DAZ associated protein 2
C7-14	10	PYSSPPTAV	H-2-Kd	332	Ncoa1	c.C3026T	p.G1009V	nuclear receptor coactivator 1
C7-15	8	EPPDHLTI	H-2-Dd	2660	Cep170	c.A4151C	p.H1384P	DAZ associated protein 2
C7-16	8	RPAPKSFL	H-2-Ld	119	Samhd1	c.A973C	p.T325P	SAM domain and HD domain, 1
C7-17	8	RGPLNLFET	H-2-Dd	2340	Plekhg5	c.G176T	p.C59F	pleckstrin homology domain containing, family G (with RhoGef domain) member 5
C7-18	9	RGPLNLFET	H-2-Dd	3519	Plekhg5	c.G176T	p.C59F	pleckstrin homology domain containing, family G (with RhoGef domain) member 5
C7-19	8	EPKQYFDL	H-2-Ld	203	Tjp1	c.A3578T	p.Q1193L	tight junction protein 1
C7-20	8	DSPYQPKY	H-2-Dd	2865	Trim12c	c.A1193C	p.H398P	tripartite motif-containing 12C
C7-21	9	SYLSAGMV	H-2-Kd	53	Slc37a2	c.C343A	p.R1155	solute carrier family 37 (glycerol-3-phosphate transporter), member 2
C7-22	8	MPLEQWWL	H-2-Ld	135	Pfkl	c.G2210T	p.R737L	phosphofruktokinase, liver, B-type
C7-23	9	KIPFCLQSF	H-2-Dd	2320	Gls2	c.G659T	p.C220F	glutaminase 2 (liver, mitochondrial)
C7-24	9	ISPGEEMQF	H-2-Dd	1949	Timeless	c.G1923C	p.L641F	timeless circadian clock 1
C7-25	8	LGPPRSSP	H-2-Dd	2125	Sh3bp5l	c.G857C	p.R286P	SH3 binding domain protein 5 like
C7-26	8	GPPRSSPV	H-2-Dd	2437	Sh3bp5l	c.G857C	p.R286P	SH3 binding domain protein 5 like
C7-27	9	LGPPRSSPV	H-2-Dd	711	Sh3bp5l	c.G857C	p.R286P	SH3 binding domain protein 5 like
C7-28	9	KYANRSRNI	H-2-Kd	52	Kif21a	c.G1102T	p.A368S	kinesin family member 21A
C7-29	8	FAPRH5RL	H-2-Dd	2431	Zfp598	c.G881T	p.R294L	zinc finger protein 598
C7-30	8	QPPNLIGL	H-2-Dd	2728	Rbm27	c.G1379C	p.R460P	RNA binding motif protein 27
C7-31	9	WFQAMANGL	H-2-Kd	106	Strbp	c.G632T	p.R211M	spermatid perinuclear RNA binding protein
C7-32	8	CGPRRRRS	H-2-Dd	3179	Rpp25l	c.G471T	p.R157S	ribonuclease P/MRP 25 subunit-like
C7-33	9	TTPATSTTF	H-2-Dd	3370	Cnot1	c.G4025T	p.C1342F	CCR4-NOT transcription complex, subunit 1
C7-34	9	TYMSSVCWL	H-2-Kd	22	Siae	c.G580T	p.A194S	sialic acid acetyltransferase
C7-35	9	CGPLKLLVH	H-2-Dd	1423	Supv311	c.C710T	p.A237V	suppressor of var1, 3-like 1 (S. cerevisiae)
C7-36	9	TIMVIVFFL	H-2-Ld	790	H2-DMa	c.G740T	p.G247V	histocompatibility 2, class II, locus DMA
C7-37	8	NYRPVALL	H-2-Kd	1674	Pten	c.G559A	p.D187N	phosphatase and tensin homolog
C7-38	8	RMPSSAAI	H-2-Dd	3632	Nfe2l2	c.A865C	p.S289R	nuclear factor, erythroid derived 2, like 2
C7-39	8	PAPKSFLY	H-2-Dd	3642	Samhd1	c.A973C	p.T325P	SAM domain and HD domain, 1
C7-40	10	VYKVVGSSTA	H-2-Kd	1466	Exoc1	c.C305G	p.A102G	exocyst complex component 1
C7-41	8	FPTDCHSI	H-2-Ld	482	Atg2b	c.G1858A	p.V620I	autophagy related 2B
C7-42	8	LGPEGYSV	H-2-Dd	3825	Cyhr1	c.G335A	p.C112Y	cysteine and histidine rich 1
C7-43	10	CYRRASSCSL	H-2-Kd	164	Ripk2	c.G1219T	p.D407Y	receptor (TNFRSF)-interacting serine-threonine kinase 2
C7-44	10	SYLSAGMVL	H-2-Kd	137	Slc37a2	c.C343A	p.R1155	solute carrier family 37 (glycerol-3-phosphate transporter), member 2
C7-45	9	SPGEEMQFL	H-2-Ld	154	Timeless	c.G1923C	p.L641F	timeless circadian clock 1
C7-46	10	LYLPMVQSV	H-2-Kd	547	Dazap2	c.C224T	p.A75V	DAZ associated protein 2
C7-47	8	RPVNIMEV	H-2-Ld	749	Tbc1d19	c.G1465C	p.A489P	TBC1 domain family, member 19
C7-48	9	FPLQGLHKL	H-2-Ld	23	Tbc1d1	c.G1151T	p.C384F	TBC1 domain family, member 1
C7-49	8	LPALASNL	H-2-Ld	672	Zfp467	c.C1715T	p.P572L	zinc finger protein 467
C7-50	8	KPLINRHL	H-2-Ld	864	Snx19	c.C2845A	p.Q949K	sorting nexin 19

(Continued on next page)

Table 1. (Continued)

ID	length	peptide	Allele	IC50 (nM)	Symbol	n Change	a.a.Change	Entrez gene name
C7-51	10	CGPLKLLVHE	H-2-Dd	3255	Supv311	c.C710T	p.A237V	suppressor of var1, 3-like 1 (S. cerevisiae)
C7-52	8	SPGEEMQF	H-2-Ld	755	Timeless	c.G1923C	p.L641F	timeless circadian clock 1
C7-53	8	IPSHYTEL	H-2-Ld	631	Atg2b	c.G1858A	p.V620I	autophagy related 2B
C7-54	9	HLPRNSAMI	H-2-Dd	3499	Dcp1a	c.A1075G	p.T359A	decapping mRNA 1A
C7-55	9	NPGAAEPPL	H-2-Ld	586	Chd8	c.G797	p.G266E	chromodomain helicase DNA binding protein 8
C7-56	8	SDVNAFNL	H-2-Ld	1046	Trabd	c.G118A	p.D40N	Trab domain containing
C7-57	9	RAQTQPPL	H-2-Ld	1120	Rbm27	c.G1379C	p.R460P	RNA binding motif protein 27

n Change: nucleotide substitution and position.

a.a.Change: amino acid substitution and position.

(Fig. 6A). In addition, we confirmed that a significant increase in CXCL9 mRNA levels was observed only following the addition of mSnd1 (Fig. 6B). The data obtained from IFN $\gamma$  ICS and ELISPOT assays also strongly supported our assertion that the immune responses to mSnd1, not to wSnd1, is elicited in CMS7 tumor-bearing mice and augmented by antibody treatment (Fig. 6C and D). It should also be noted that in the case of untreated mouse group, the specific immune response to this neo-epitope could be detected by our method, but not by the IFN $\gamma$  ICS method (Fig. 6C).

To assess the immunogenicity of the mSnd1 neo-epitope, we immunized mice with this peptide twice, 14 and 7 d before the CMS7 tumor challenge. At day 0, CMS7 cells were subcutaneously injected to the mice. As shown in Fig. 6E, mice immunized with the mSnd1 peptide developed resistance to the CMS7 challenge, whereas no tumor immunity was observed in any of the other groups, except for the antibody-treated group that showed complete reduction of tumor growth.

## Discussion

The chemokines CXCL9, 10, and 11 play crucial roles in a wide variety of inflammatory immune responses,<sup>24,25</sup> including tumor immunity. Indeed, in many types of malignancies, there is close correlation between higher expression of CXCR3 ligands at both the mRNA and protein levels and a higher number of tumor-infiltrating T lymphocytes.<sup>26-29</sup> In addition, recent clinical studies have shown that the expression of these chemokines in tumor tissue before treatment was positively associated with a favorable clinical response to immunotherapies, such as a cancer vaccine targeting MAGE-A3,<sup>30</sup> an immunogenic cancer/testis antigen, and an immunotherapy using an anti-CTLA-4 antibody for melanoma patients.<sup>31</sup> These results are not unexpected, considering that IFN $\gamma$ , the pivotal player in anti-tumor immune response, triggers the production of these chemokines and thereby recruits CXCR3<sup>+</sup> immune effector cells, such as Th1 cells, NK cells, and activated CD8<sup>+</sup> T cells, to tumor sites.

The *in vitro* data of our present study indicate that CXCR3 ligands appeared to be sensitive indicators of specific immune responses, which are consistent with the results reported by Chakera et al.<sup>14</sup> In particular, we often observed a significant increase in CXCR3 ligand mRNA levels, which was however, not accompanied by an increase in IFN $\gamma$  mRNA levels. Likewise, we observed a rapid increase of CXCR3 ligands at the

protein level, which was substantially diminished by blocking IFN $\gamma$  signaling, although no measurable IFN $\gamma$  was detected in the same culture medium. These data exemplify the amplification of IFN $\gamma$  signals as a prominent property of CXCR3 ligands. In conclusion, we have shown that the utilization of CXCR3 ligand mRNA as a sensitive and specific immune response indicator is a promising strategy.

To examine the feasibility of this approach for identifying immunogenic neo-epitopes, we used a murine CMS5 tumor model since our group has previously identified a mutated ERK2-derived neo-epitope (mERK2-9m) as a tumor rejection antigen of CMS5 tumors, by cDNA cloning from a CD8<sup>+</sup> T-cell clone (C18), established from draining lymph node cells of CMS5 tumor-bearing mice.<sup>18</sup> Moreover, adoptive transfer of CD8<sup>+</sup> T cells from DUC18 mice, expressing a TCR  $\alpha/\beta$  gene derived from clone C18, has been shown to potently eradicate established CMS5 tumors.<sup>19</sup> However, an immune response to this epitope could not be detected by our approach in untreated mice. The cause of this unexpected result could be the low antigenicity of this peptide. Consistently with this speculation, another group recently reported that specific immune responses to this epitope were hardly detectable even after immunization with this peptide.<sup>32</sup> However, the fact that our approach successfully detected this specific immune response following the checkpoint antibody treatment encouraged us to validate our approach for identifying other neo-epitopes with higher antigenicity in another mouse model.

As shown in Fig. 6, we successfully detected CD8<sup>+</sup> T-cell immune response to a single neo-epitope (YAPCRGEF) derived from mutated Snd1 in the CMS7 tumor model even without the checkpoint antibody treatment. Furthermore, we observed that the antibody treatment augmented the immune response and resulted in successful detection of the immune response to the neo-epitope (YAPCRGEF) but not its wild-type counterpart (YAPRRGEF) by the IFN $\gamma$  ICS method (Fig. 6B-D). These data clearly demonstrate the higher sensitivity of our method than that of IFN $\gamma$  ICS. In addition, as shown in Fig. 3A, the sensitivity of this method seems to be almost equal to that of IFN $\gamma$  ELISPOT assay, since we were able to detect the existence of approximately 20 antigen-specific CD8<sup>+</sup> T cells among  $1 \times 10^6$  splenic cells (0.002% antigen-specific CD8<sup>+</sup> T cells/whole cells). However, under different conditions, our approach might be more sensitive compared with the IFN $\gamma$  ELISPOT assay, since we could not detect specific immune responses to mERK2-9m or the mutated Snd1-derived neo-

epitope by the IFN $\gamma$  ELISPOT assay, in antibody-treated CMS5 tumor-bearing mice (Fig. 5D) or in antibody-untreated CMS7 tumor-bearing mice (data not shown), respectively. Further investigation is required to clarify this point.

Contrary to our expectations, our data show that we could detect an immune response to only one neo-epitope in the CMS7 tumor model. One major reason might stem from the limitations of *in silico* technics for the prediction of

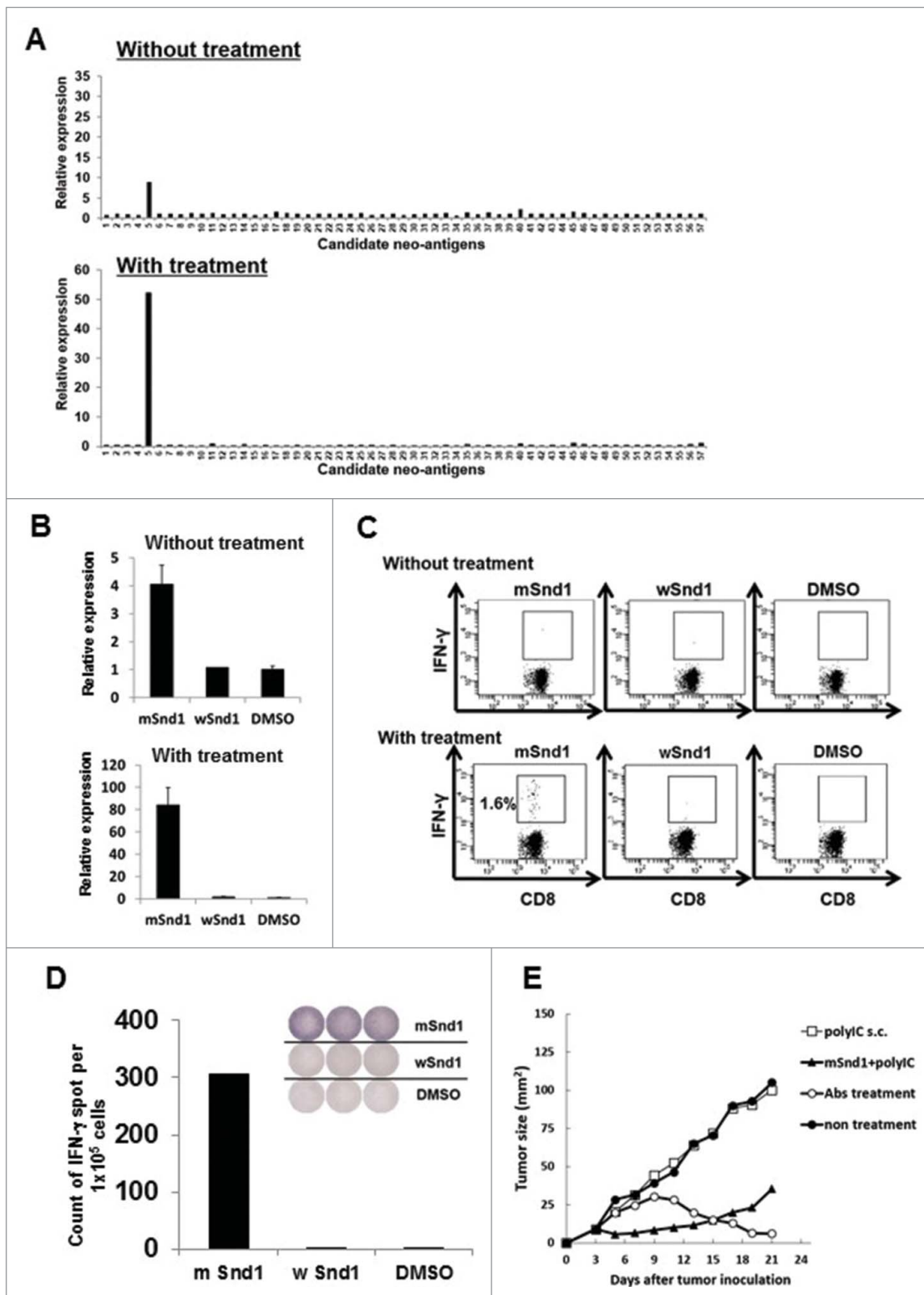


Figure 6. (For Figure legend see page 11).

immunogenic neo-epitopes. Although the list of our candidate neo-epitope peptides was based on the binding strength to H-2 alleles, selection of candidate neo-epitopes according to different criteria may improve the outcome, as proposed by another group.<sup>32</sup>

Personalized cancer vaccines using neo-epitopes encoded by an individual's tumor could be a promising strategy for the treatment of cancer patients. In the clinical setting, the quick and accurate identification of immunogenic neo-epitopes is necessary before the immunotherapy treatment and therefore, our simple and quick approach is promising. We are currently investigating whether our approach is applicable for the identification of immunogenic neo-epitopes using PBMC from cancer patients.

In conclusion, we hope that our novel method would prove useful for the identification of neo-antigens, which show therapeutic potential.

## Materials and methods

### Ethics statement (human samples)

Written informed consents were obtained from the one patient and healthy volunteers according to the guidelines of the Declaration of Helsinki. The experimental protocol was approved by the Institutional Review Board at the Mie University School of Medicine.

### Ethics statement (mouse experiments)

All mice were housed under specific pathogen free conditions and used at 8–10 weeks of age. All animal experiments were conducted using protocols approved by the Animal Care and Use Committee at the Mie University Life Science Center.

### Animal studies

Female BALB/c mice were purchased from the Shizuoka Animal Laboratory Center (Shizuoka, Japan). DUC18 mice, transgenic for  $\alpha/\beta$ -TCR reactive with the H-2K<sup>d</sup>-restricted mERK2<sub>136–144</sub>, were established as described previously.<sup>18</sup>

### Antibodies

All fluorescence-conjugated mAbs, including anti-human CD8<sup>+</sup> (HIT8a), were purchased from BioLegend (San Diego, CA, USA). Anti-human CD119 (IFN $\gamma$  receptor  $\alpha$  chain, GIR-

208) mAb, anti-human IFN $\gamma$  (NIB42) mAb, and mouse IgG1 isotype control were purchased from BioLegend. Anti-human CD3 (OKT3) mAb was purchased from BD Biosciences (San Jose, CA, USA). Anti-mouse PD-1 (RMP1–14), anti-mouse CTLA-4 (9D9) and anti-mouse GITR (DTA-1) mAbs were produced from hybridomas and were purified by protein G columns.

### Cell lines

CT26 is a colon epithelial tumor cell line derived from intrarectal injections of N-nitroso-N-methylurethane into BALB/c mice.<sup>33</sup> CMS5 and CMS7 are 3-methylcholanthrene-induced sarcoma cell lines of BALB/c origin.<sup>34</sup> NY-ESO-1 expressing human melanoma cell line 397mel was a kind gift from Dr. Y. Kawakami (Keio University, Tokyo, Japan). 397mela0201 was established by transfecting plasmid DNA encoding HLA-A0201 into 397mel cells. All tumor lines were cultured in RPMI-1640 medium supplemented with 10% heat-inactivated Fetal Calf Serum (FCS) (Biowest, Kansas, USA), 50  $\mu$ M 2-mercaptoethanol (2-ME), and 0.2 mg/mL glutamine.

### Cytokine/chemokine measurements

The levels of 48 kinds of human cytokines and chemokines in culture supernatants were determined using Bio-Plex kits (Bio-Rad, Hercules, CA, USA) according to the manufacturer's instructions. The analytes included IL-1 $\alpha$ , IL-1 $\beta$ , IL-1Ra, IL-2, IL-2R $\alpha$ , IL-3, IL-4, IL-5, IL-6, IL-7, IL-8, IL-9, IL-10, IL-12 (p40), IL-12(p70), IL-13, IL-15, IL-16, IL-17, IL-18, eotaxin, FGF basic, G-CSF, GM-CSF, IFN $\gamma$ , MCP-1, CCL3, CCL4, CCL5, PDGF-BB, CTACK, GRO- $\alpha$ , HGF, IFN $\alpha$ 2, LIF, MCP3, M-CSF, MIF, CXCL9, CXCL10,  $\beta$ -NGF, SCF, SCGF- $\beta$ , SDF-1 $\alpha$ , TNF- $\alpha$ , TNF- $\beta$ , TRAIL, and VEGF. In some experiments, the levels of human CXCL9, CXCL10, and IFN $\gamma$  were analyzed using quantitative human DuoSet ELISA kits (R&D Systems, Minneapolis, MN).

### Cell staining

For intracellular cytokine staining, splenocytes ( $1 \times 10^6$ ) were incubated with 50  $\mu$ M synthetic peptide or DMSO for 15 min at room temperature, and subsequently with GolgiPlug (BD Bioscience) for 4 h. The cells were stained with a CD8 $\alpha$ -specific mAb for 15 min at 4  $^{\circ}$ C. After permeabilization and fixation

**Figure 6.** (See previous page). Successful identification of an immunogenic neo-epitope encoded by mouse sarcoma CMS7. (A) After subcutaneous inoculation with CMS7 cells, mice were randomly divided into two groups. One group was left untreated, and the other was administered intraperitoneally with anti-CTLA-4, anti-PD-1 and anti-GITR mAbs on days 7, 9, and 11. Both mouse groups were sacrificed at day 21 and splenic cell suspensions were prepared from pooled spleens ( $n = 3$  per experiment). Splenic cells from untreated (upper) or treated mice (lower) were incubated with each panel of neo-epitope peptides for 5 h and the fold increase in CXCL9 mRNA levels compared with DMSO was quantified. One representative data set out of three independent experiments is shown. (B) Splenic cells from untreated (upper) or treated mice (lower) were incubated with mutated Snd1 peptide, its wild-counterpart or DMSO as a control for 5 h and the fold increase in CXCL9 mRNA levels compared with DMSO was quantified. (C) Splenic cells from untreated (upper) or treated mice (lower) were incubated with mutated Snd1 peptide, its wild-counterpart or DMSO as a control for 15 min at room temperature and subsequently with GolgiPlug for 4 h. Following stimulation, cells were stained for cell surface CD8<sup>+</sup> and intracellular IFN $\gamma$ . Representative dot plots gated on CD8<sup>+</sup> splenic T cells are shown. The number indicates the percentage of CD8<sup>+</sup> IFN $\gamma$ <sup>+</sup> T cells. These experiments were repeated three times with similar results. (D) CD8<sup>+</sup> splenic T cells were obtained from antibody-treated mice pooled spleens by positive enrichment using the MACS system, and were stimulated *in vitro* with mutated Snd1-pulsed CD8<sup>-</sup> splenic cells. Cultured CD8<sup>+</sup> splenic T cells were subjected to ELISPOT assays 10 d later. The target cells were CD8<sup>-</sup> splenic cells pulsed with mutated Snd1 peptide, or its wild counterpart. Splenic cells pulsed with DMSO were used as control targets. (E) Age-matched female BALB/c mice were inoculated with CMS7 at day 0 following two injections (at days -14 and -7) with mSnd1 peptide and poly (I:C) formulated in PBS or poly (I:C) alone using prophylactic schedules. The tumor size was monitored three times a week. Each group consisted of five mice. Mice without any immunization and mice treated by the co-administration of antibodies (anti-CTLA-4/PD-1/GITR Abs) at days 7, 9, 11 served as a negative control group and a positive control group, respectively.



using a Cytofix/Cytoperm kit (BD Biosciences) according to manufacturer's instructions, the cells were stained intracellularly using an allophycocyanin-conjugated anti-IFN $\gamma$  mAb.

### Enzyme-linked immunospot (ELISPOT) assay

Murine IFN $\gamma$  ELISPOT assays were performed as described previously.<sup>35</sup> Briefly, 96-well nitrocellulose ELISPOT plates (MAHA S4510; Millipore, Bedford, MA) were coated with 2  $\mu$ g/mL anti-mouse IFN $\gamma$  mAb (mAb, clone R4-6A2; PharMingen, San Diego, CA) overnight at 4 °C, washed with 0.05% Tween 20 in PBS (PBS/Tween) and blocked with FCS-containing culture medium for 2 h at 37 °C. Cultured CD8<sup>+</sup> T cells (1  $\times$  10<sup>5</sup> per well) and mutated Snd1 peptide-pulsed CD8<sup>-</sup> splenic cells (1  $\times$  10<sup>6</sup> per well) were plated at a final volume of 200  $\mu$ L per well, and were incubated for 18 h at 37 °C in a CO<sub>2</sub> incubator. Following a thorough wash with PBS/Tween, 1.25  $\mu$ g/mL biotinylated anti-mouse IFN $\gamma$  mAb (PharMingen) was added, and the plate was incubated overnight at 4 °C, washed with PBS/Tween, and further incubated with 1  $\mu$ g/mL streptavidin-alkaline phosphatase conjugate (Mabtech, Nacka, Sweden) in 100  $\mu$ L PBS per well for 90 min at room temperature. Following three washes with PBS/Tween, the staining was performed with an alkaline phosphatase conjugate substrate kit (BioRad), the reaction was stopped by adding distilled water, and the stained spots were counted using an ELISPOT Plate Reader (ImmunoSpot, CTL-Europe GmbH) after drying.

### Peptides

The EB virus-derived peptides EBNA3A<sub>246-254</sub> (RYSIFFDYM), EBNA3A<sub>240-259</sub> (VQSCNPRYSIFFDYMAIHRS), AH-1 (SPSYVYHQF), the mutated ERK2-derived peptide (mERK2-9m; QYIHSANVL), the non-mutated ERK2-derived peptide (wERK2-9m; KYIHSANVL),<sup>18</sup> the mutated Snd1-derived peptide (mSnd1; YAPCRGEF), the non-mutated Snd1-derived peptide (wSnd1; YAPRRGEF), and 17 overlapping peptides spanning the NY-ESO-1 protein (Table S1) were synthesized at a purity higher than 80% from Invitrogen (Carlsbad, CA, USA). All peptides were dissolved in DMSO at a concentration of 10 mM and stored in aliquots at -80 °C before use.

### Immunization

The complex of cholesterol-bearing hydrophobized pullulan (CHP) and NY-ESO-1 protein (CHP-NY-ESO-1) was provided by ImmunoFrontier, Inc. (Tokyo, Japan).<sup>20</sup> CHP-NY-ESO-1 complex vaccines were subcutaneously injected into the back of BALB/c mice at a dose of 50  $\mu$ g, twice, at a 1-week interval. Following 7 d from the second vaccination, spleen cells were harvested for analysis. In another experiment, before CMS7 tumor challenge, 200  $\mu$ g mSnd1 peptide and 50  $\mu$ g poly(I:C) formulated in PBS (200  $\mu$ L total volume) were subcutaneously injected into the back of BALB/c mice, twice, at a 1-week interval.

### Preparation of murine splenic cells

Mice spleens were mashed with a microscope slide, treated with ammonium chloride-potassium (ACK) and filtrated with Cell Trics<sup>®</sup> 30  $\mu$ m (Sysmex Partec, Kobe, Japan). Single cell suspensions from pooled spleen were cultured in 96-well V-bottom plates at a density of 5  $\times$  10<sup>6</sup> cells/mL, with the appropriate peptide. In some experiments, CD8<sup>+</sup> splenic T cells were obtained by positive enrichment using the MACS system (Miltenyi Biotec, Bergisch Gladbach, Germany). Flow cytometry confirmed that the T-cell fractions contained more than 95% CD8<sup>+</sup> T cells.

### Preparation of human cell populations

Peripheral blood mononuclear cells (PBMC) were isolated from fresh heparinized venous blood samples with density-gradient centrifugation in Ficoll-Paque PLUS (GE Healthcare, Buckinghamshire, UK). CD8<sup>+</sup> cell-depleted or CD14<sup>+</sup> cell-depleted subsets were obtained from PBMC using FACSaria (BD Biosciences).

### T-cell transduction

PBMC obtained from healthy volunteers were stimulated using a plate-coated anti-CD3 antibody and RetroNectin (Takara Bio, Inc., Otsu, Japan) in the presence 600 IU/mL of recombinant IL-2. Proliferating lymphocytes were transduced with a retrovirus encoding NY-ESO-1<sub>p157-165</sub>/HLA-A0201-specific TCR- $\alpha$  and - $\beta$  chains, and were expanded further *in vitro*. Ten days after transduction, CD8<sup>+</sup> T cells expressing NY-ESO-1-specific TCR, determined by the specific tetramer, were sorted using FACSaria (BD Biosciences).

### Blocking assay

Human lymphocytes (1  $\times$  10<sup>6</sup>) were cultured in 200  $\mu$ L X-VIVO<sup>™</sup>15 (Lonza, Walkersville, MD, USA) in 96-well V-bottom plates in the presence of anti-human CD119, anti-human IFN $\gamma$ , or mouse IgG1 isotype control (final 10  $\mu$ g/mL) for 1 h before the addition of the EBNA3A<sub>246-254</sub> peptide.

### Next generation sequencing and data analysis

DNA extracted from CMS7 tumor cells or BALB/c tails by conventional methods was subjected to exome capturing using the SureSelectXT mouse exon kit (Agilent Technologies, Santa Clara, CA, USA). Exome capture libraries were subsequently sequenced with a HiSeq2000 (Illumina, CA) sequencing system, using the Illumina V3 kit (Riken Genesis Co., Ltd.). From each library, 20M (2  $\times$  150 bp) exome reads were sequenced. RNA samples extracted from CMS7 tumor cells were used to generate RNA-seq libraries, which were sequenced by Hokkaido System Science Co., Ltd., with an Illumina HiSeq 2000 (Illumina) sequencing system. From each library, 30M (2  $\times$  100 bp) RNA fragments were sequenced. Whole exome sequence reads were aligned to the mm9 reference sequence using the Burrows-Wheeler Aligner (BWA) software.<sup>36</sup> Somatic single nucleotide variants (SNVs) were detected from read

count comparisons between normal and tumor samples using the Fisher exact test, and variants whose  $p$ -value was less than  $10^{-10}$  were considered as statistically significant. From the identified SNVs, we extracted only non-synonymous SNVs. We also aligned sequence reads from RNA-seq libraries to mm9 using the Bowtie algorithm of the TopHat software<sup>37</sup> to confirm whether the variants detected in whole exome sequencing were indeed transcribed to RNA. Based on the aligned RNA sequence reads, the candidate variants from whole exome sequencing were tested by the Fisher exact test, and variants with a  $p$ -value less than  $10^{-10}$  were considered as transcribed SNVs.

### Selection of candidate neo-epitopes

To identify potential neo-epitopes that could bind murine MHC class I, we used the IEDB Analysis Resource (<http://www.iedb.org/>). Briefly, all candidate neo-epitopes (8–10-mer) containing missense mutations were analyzed *in silico* for their binding affinities to either H-2K<sup>d</sup>, H-2D<sup>d</sup> or H-2L<sup>d</sup> molecules based on the IEDB recommended method (Consensus) consisting of the Artificial Neural Network (ANN), the Stabilized Matrix Method (SMM), and the Scoring Matrices derived from Combinatorial Peptide Libraries (Comblib\_Sidney2008) algorithms.<sup>38</sup> Based on percentile rank ( $\leq 0.6$ ) and IC<sub>50</sub> ( $< 4,000$  nM) values (Table 1), we selected 57 different candidate neo-epitopes for CMS7 cells.

### Reverse transcription quantitative polymerase chain reaction (RT-qPCR)

We performed the experiment protocol described below, referring to a previous report.<sup>14</sup> Total RNA from cultured cells was extracted using an RNA Blood Mini Kit (Qiagen, Hilden, Germany) and was reverse-transcribed into first-strand cDNA (cDNA) using a QuantiTect Reverse Transcription Kit (Qiagen). Quantitative PCR was performed using a Step One Plus (Applied Biosystems, Carlsbad, CA, USA) according to the manufacturer's protocol. Primers and probes were selected from the ABI TaqMan Gene Expression Assay catalog (for human targets: CXCL9, Hs00171065\_m1; CXCL10, Hs01124251\_g1; CXCL11, Hs04187682\_g1; IFN $\gamma$ , Hs00989291\_m1; TNF $\alpha$ , Hs01113624\_g1; CCL3, Hs00234142\_m1; CCL4, Hs00237011\_m1; CCL5, Hs00174575\_m1; TRAIL, Hs00921974\_m1; and IL-13, Hs00174379\_m1; for mouse targets: CXCL9, Mm00434946\_m1; CXCL10, Mm00445235\_m1; CXCL11, and Mm00444662\_m1). Expression of each gene was normalized to that of *GAPDH*. Fold change was determined by the  $\Delta\Delta C_t$  method. Each experiment was performed in triplicate.

### Statistical analysis

Statistical significance was evaluated using the unpaired Student's  $t$ -test and  $p$  values less than 0.05 were considered as statistically significant.

### Disclosure of potential conflicts of interest

No potential conflicts of interest were disclosed.

### Acknowledgment

The authors thank Dr. Toshitada Takahashi for helpful discussions.

### Funding

This work was supported by Grants-in-Aid for Scientific Research from the Japan Society for the Promotion of Science (16K07168).

### References

- Matthew MG, Xiuli Z, Heiko S, Etienne C, Jeffrey PW, Takuro N, Yulia I, Jasreet H, Cora DA, Willem-Jan K et al. Checkpoint blockade cancer immunotherapy targets tumour-specific mutant antigens. *Nature* 2014; 515:577-81; PMID:25428507; <https://doi.org/10.1038/nature13988>
- John CC, Sebastian K, Jan D, Martin L, Niels van de R, Jos de G, Abderraouf S, Mustafa D, Sebastian B, Claudia P et al. Exploiting the mutanome for tumor vaccination. *Cancer Res* 2012; 72:1081-91; PMID:22237626; <https://doi.org/10.1158/0008-5472.CAN-11-3722>
- Brown SD, Warren RL, Gibb EA, Martin SD, Spinelli JJ, Nelson BH, Holt RA. Neo-antigens predicted by tumor genome meta-analysis correlate with increased patient survival. *Genome Res* 2014; 24:743-50; PMID:24782321; <https://doi.org/10.1101/gr.165985.113>
- Snyder A, Makarov V, Merghoub T, Yuan J, Zaretsky JM, Desrichard A, Walsh LA, Postow MA, Wong P, Ho TS et al. Genetic basis for clinical response to CTLA-4 blockade in melanoma. *N Engl J Med* 2014; 371:2189-99; PMID:25409260; <https://doi.org/10.1056/NEJMoa1406498>
- van Rooij N, van Buuren MM, Philips D, Velds A, Toebes M, Heemskerk B, van Dijk LJ, Behjati S, Hilkmann H, El Atmioui D et al. Tumor exome analysis reveals neoantigen-specific T-cell reactivity in an ipilimumab-responsive melanoma. *J Clin Oncol* 2013; 31:e439-42; PMID:24043743; <https://doi.org/10.1200/JCO.2012.47.7521>
- Hodi FS, O'Day SJ, McDermott DF, Weber RW, Sosman JA, Haanen JB, Gonzalez R, Robert C, Schadendorf D, Hassel JC et al. Improved survival with ipilimumab in patients with metastatic melanoma. *N Engl J Med* 2010; 363:711-23; PMID:20525992; <https://doi.org/10.1056/NEJMoa1003466>
- Rizvi NA, Hellmann MD, Snyder A, Kvistborg P, Makarov V, Havel JJ, Lee W, Yuan J, Wong P, Ho TS et al. Cancer immunology. Mutational landscape determines sensitivity to PD-1 blockade in non-small cell lung cancer. *Science* 2015; 348:124-8; PMID:25765070; <https://doi.org/10.1126/science.aaa1348>
- Le DT, Uram JN, Wang H, Bartlett BR, Kemberling H, Eyring AD, Skora AD, Luber BS, Azad NS, Laheru D et al. PD-1 blockade in tumors with mismatch-repair deficiency. *N Engl J Med* 2015; 372:2509-20; PMID:26028255; <https://doi.org/10.1056/NEJMoa1500596>
- Robbins PF, Lu YC, El-Gamil M, Li YF, Gross C, Gartner J, Lin JC, Teer JK, Cliften P, Tycksen E et al. Mining exomic sequencing data to identify mutated antigens recognized by adoptively transferred tumor-reactive T cells. *Nat Med* 2013; 19:747-52; PMID:23644516; <https://doi.org/DOI:10.1038/nm.3161>
- Tran E, Turcotte S, Gros A, Robbins PF, Lu YC, Dudley ME, Wunderlich JR, Somerville RP, Hogan K, Hinrichs CS et al. Cancer immunotherapy based on mutation-specific CD4<sup>+</sup> T cells in a patient with epithelial cancer. *Science* 2014; 344:641-5; PMID:24812403; <https://doi.org/10.1126/science>
- Gros A, Parkhurst MR, Tran E, Pasetto A, Robbins PF, Ilyas S, Prickett TD, Gartner JJ, Crystal JS, Roberts IM et al. Prospective identification of neoantigen-specific lymphocytes in the peripheral blood of melanoma patients. *Nat Med* 2016; 22:433-8; PMID:26901407; <https://doi.org/10.1038/nm.4051>
- Yadav M, Jhunjhunwala S, Phung QT, Lupardus P, Tanguay J, Bum-baca S, Franci C, Cheung TK, Fritsche J, Weinschenk T et al. Predicting immunogenic tumour mutations by combining mass spectrometry and exome sequencing. *Nature* 2014; 515:572-6; PMID:25428506; <https://doi.org/10.1038/nature14001>
- Bakker AH, Hoppes R, Linnemann C, Toebes M, Rodenko B, Berkers CR, Hadrup SR, van Esch WJ, Heemskerk MH, Ovaa H et al. Conditional MHC class I ligands and peptide exchange technology for the

- human MHC gene products HLA-A1, -A3, -A11, and -B7. *Proc Natl Acad Sci USA* 2008; 105:3825-30; PMID:18308940; <https://doi.org/10.1073/pnas.0709717105>
14. Chakera A, Bennett SC, Cornall RJ. A whole blood monokine-based reporter assay provides a sensitive and robust measurement of the antigen-specific T cell response. *J Transl Med* 2011; 9:143; PMID:21871084; <https://doi.org/10.1186/1479-5876-9-143>
  15. Chen YT, Scanlan MJ, Sahin U, Türeci O, Gure AO, Tsang S, Williamson B, Stockert E, Pfreundschuh M, Old LJ. A testicular antigen aberrantly expressed in human cancers detected by autologous antibody screening. *Proc Natl Acad Sci USA* 1997; 94:1914-8; PMID:9050879
  16. Chen JL, Dunbar PR, Gileadi U, Jäger E, Gnjatich S, Nagata Y, Stockert E, Panicali DL, Chen YT, Knuth A et al. Identification of NY-ESO-1 peptide analogues capable of improved stimulation of tumor-reactive CTL. *J Immunol* 2000; 165:948-55; PMID:10878370; <https://doi.org/10.4049/jimmunol.165.2.948>
  17. Burrows SR, Gardner J, Khanna R, Steward T, Moss DJ, Rodda S, Suhrbier A. Five new cytotoxic T cell epitopes identified within Epstein-Barr virus nuclear antigen 3. *J Gen Virol* 1994; 75:2489-93; PMID:7521394; <https://doi.org/10.1099/0022-1317-75-9-2489>
  18. Ikeda H, Ohta N, Furukawa K, Miyazaki H, Wang L, Kuribayashi K, Old LJ, Shiku H. Mutated mitogen-activated protein kinase: a tumor rejection antigen of mouse sarcoma. *Proc Natl Acad Sci USA* 1997; 94:6375-9; PMID:9177225; <https://doi.org/10.1073/pnas.94.12.6375>
  19. Hanson HL, Donermeyer DL, Ikeda H, White JM, Shankaran V, Old LJ, Shiku H, Schreiber RD, Allen PM. Eradication of established tumors by CD8+ T cell adoptive immunotherapy. *Immunity* 2000; 13:265-76; PMID:10981969; [https://doi.org/10.1016/S1074-7613\(00\)00026-1](https://doi.org/10.1016/S1074-7613(00)00026-1)
  20. Kageyama S, Wada H, Muro K, Niwa Y, Ueda S, Miyata H, Takiguchi S, Sugino SH, Miyahara Y, Ikeda H et al. Dose-dependent effects of NY-ESO-1 protein vaccine complexed with cholesteryl pullulan (CHP-NY-ESO-1) on immune responses and survival benefits of esophageal cancer patients. *J Transl Med* 2013; 11:246; PMID:24093426; <https://doi.org/10.1186/1479-5876-11-246>
  21. Muraoka D, Nishikawa H, Noguchi T, Wang L, Harada N, Sato E, Luescher I, Nakayama E, Kato T, Shiku H. Establishment of animal models to analyze the kinetics and distribution of human tumor antigen-specific CD8+ T cells. *Vaccine* 2013; 31:2110-8; PMID:23499606; <https://doi.org/10.1016/j.vaccine.2013.02.056>
  22. Dengel LT, Norrod AG, Gregory BL, Clancy-TE, Burdick MD, Strieter RM, Slingluff CL Jr, Mullins DW. Interferons induce CXCR3-cognate chemokine production by human metastatic melanoma. *J Immunother* 2010; 33:965-74; PMID:20948440; <https://doi.org/10.1097/CJI.0b013e3181fb045d>
  23. Huang AY, Gulden PH, Woods AS, Thomas MC, Tong CD, Wang W, Engelhard VH, Pasternack G, Cotter R, Hunt D, Pardoll DM, Jaffee EM. The immunodominant major histocompatibility complex class I-restricted antigen of a murine colon tumor derives from an endogenous retroviral gene product. *Proc Natl Acad Sci USA* 1996; 93:9730-5; PMID:8790399; <https://doi.org/10.1073/pnas.93.18.9730>
  24. Lacotte S, Brun S, Muller S, Dumortier H. CXCR3, inflammation, and autoimmune diseases. *Ann NY Acad Sci* 2009; 1173:310-7; PMID:19758167; <https://doi.org/10.1111/j.1749-6632.2009.04813.x>
  25. Wendel M, Galani IE, Suri-PE, Cerwenka A. Natural killer cell accumulation in tumors is dependent on IFN-gamma and CXCR3 ligands. *Cancer Res* 2008; 68:8437-45; PMID:18922917; <https://doi.org/10.1158/0008-5472.CAN-08-1440>
  26. Ohtani H, Jin Z, Takegawa S, Nakayama T, Yoshie O. Abundant expression of CXCL9 (MIG) by stromal cells that include dendritic cells and accumulation of CXCR3+ T cells in lymphocyte-rich gastric carcinoma. *J Pathol* 2009; 217:21-31; PMID:18980207; <https://doi.org/10.1002/path.2448>
  27. Harlin H, Meng Y, Peterson AC, Zha Y, Tretiakova M, Slingluff C, McKee M, Gajewski TF. Chemokine expression in melanoma metastases associated with CD8+ T-cell recruitment. *Cancer Res* 2009; 69:3077-85; PMID:19293190; <https://doi.org/10.1158/0008-5472.CAN-08-2281>
  28. Kondo T, Nakazawa H, Ito F, Hashimoto Y, Osaka Y, Futatsuyama K, Toma H, Tanabe K. Favorable prognosis of renal cell carcinoma with increased expression of chemokines associated with a Th1-type immune response. *Cancer Sci* 2006; 97:780-6; PMID:16863511; <https://doi.org/10.1111/j.1349-7006.2006.00231.x>
  29. Kunz M, Toksoy A, Goebeler M, Engelhardt E, Bröcker E, Gillitzer R. Strong expression of the lymphoattractant C-X-C chemokine Mig is associated with heavy infiltration of T cells in human malignant melanoma. *J Pathol* 1999; 189:552-8; PMID:10629557; [https://doi.org/10.1002/\(SICI\)1096-9896\(199912\)189:4%3c552::AID-PATH469%3e3.0.CO;2-I](https://doi.org/10.1002/(SICI)1096-9896(199912)189:4%3c552::AID-PATH469%3e3.0.CO;2-I)
  30. Ulloa-Montoya F, Louahed J, Dizier B, Gruselle O, Spiessens B, Lehmann FF, Suci S, Kruit WH, Eggermont AM, Vansteenkiste J et al. Predictive gene signature in MAGE-A3 antigen-specific cancer immunotherapy. *J Clin Oncol* 2013; 31:2388-95; PMID:23715562; <https://doi.org/10.1200/JCO.2012.44.3762>
  31. Ji RR, Chasalow SD, Wang L, Hamid O, Schmidt H, Cogswell J, Alaparthi S, Berman D, Jure-Kunkel M, Siemers NO, Jackson JR, Shahabi V. An immune-active tumor microenvironment favors clinical response to ipilimumab. *Cancer Immunol Immunother* 2012; 61:1019-31; PMID:22146893; <https://doi.org/10.1007/s00262-011-1172-6>
  32. Duan F, Duitama J, Al Seesi S, Ayres CM, Corcelli SA, Pawashe AP, Blanchard T, McMahon D, Sidney J, Sette A et al. Genomic and bioinformatic profiling of mutational neoepitopes reveals new rules to predict anticancer immunogenicity. *J Exp Med* 2014; 11:2231-48; <https://doi.org/10.1084/jem.20141308>
  33. Griswold DP, Corbett TH. A colon tumor model for anticancer agent evaluation. *Cancer* 1975; 36:2441-4; PMID:1212662; [https://doi.org/10.1002/1097-0142\(197512\)36:6%3c2441::AID-CNCR2820360627%3e3.0.CO;2-P](https://doi.org/10.1002/1097-0142(197512)36:6%3c2441::AID-CNCR2820360627%3e3.0.CO;2-P)
  34. DeLeo AB, Shiku H, Takahashi T, John M, Old LJ. Cell surface antigens of chemically induced sarcomas of the mouse. I. Murine leukemia virus-related antigens and alloantigens on cultured fibroblasts and sarcoma cells: description of a unique antigen on BALB/c Meth A sarcoma. *J Exp Med* 1977; 146:720-34; PMID:197192
  35. Power CA, Grand CL, Ismail N, Peters NC, Yurkowski DP, Bretscher PA. A valid ELISPOT assay for enumeration of ex vivo, antigen-specific, IFN-gamma-producing T cells. *J Immunol Methods* 1999; 227:99-107; PMID:10485258; [https://doi.org/10.1016/S0022-1759\(99\)00074-5](https://doi.org/10.1016/S0022-1759(99)00074-5)
  36. Li H, Durbin R. Fast and accurate short read alignment with Burrows-Wheeler transform. *Bioinformatics* 2009; 25:1754-60; PMID:19451168; <https://doi.org/10.1093/bioinformatics/btp324>
  37. Trapnell C, Pachter L, Salzberg SL. TopHat: discovering splice junctions with RNA-Seq. *Bioinformatics* 2009; 25:1105-11; PMID:19289445; <https://doi.org/10.1093/bioinformatics/btp120>
  38. Moutaftis M, Peters B, Paschetto V, Tschärke DC, Sidney J, Bui HH, Grey H, Sette A. A consensus epitope prediction approach identifies the breadth of murine T (CD8+)-cell responses to vaccinia virus. *Nat Biotechnol* 2006; 24:817-9; PMID:16767078; <https://doi.org/10.1038/nbt1215>